Mass Measurement of ^{100}Sn

M. Chartier,[1] G. Auger,[1] W. Mittig,[1] A. Lépine-Szily,[2] L. K. Fifield,[3] J. M. Casandjian,[1] M. Chabert,[1] J. Fermé,[1] A. Gillibert,[4] M. Lewitowicz,[1] M. Mac Cormick,[1] M. H. Moscatello,[1] O. H. Odland,[5] N. A. Orr,[6] G. Politi,[7] C. Spitaels,[1] and A. C. C. Villari[1]

[1]*Grand Accélérateur National d'Ions Lourds, Bld Henri Becquerel, BP 5027, 14021 Caen Cedex, France*
[2]*IFUSP-Universidade de São Paulo, C.P. 66318, 05389-970 São Paulo, Brazil*
[3]*Department of Nuclear Physics, RSPhySE, Australian National University, ACT 0200, Australia*
[4]*Commissariat à l'Energie Atomique/Département d'Astrophysique, Physique des Particules, Physique Nucleaire et d'Instrumentation Assocciée/Service de Physique Nucléaire, Centre d'Etudes Nucléaires de Saclay, 91191 Gif-sur-Yvette, France*
[5]*Universitetet i Bergen, Fysisk Institutt, Allégaten 55, 5007 Bergen, Norway*
[6]*LPC-Institut des Sciences de la Matière et du Rayonnement, Bld du Maréchal Juin, 14050 Caen Cedex, France*
[7]*Dip. di Fisica, Universitá di Catania, Corso Italia 57, 95125 Catania, Italy*

(Received 29 April 1996)

Secondary ions of ^{100}Ag, ^{100}Cd, ^{100}In, and ^{100}Sn were produced via the fusion-evaporation reaction ^{50}Cr + ^{58}Ni at an energy of 51 MeV/nucleon, and were accelerated simultaneously in the second cyclotron of GANIL. About 10 counts were observed from the production and acceleration of ^{100}Sn^{22+}. The masses of ^{100}Cd, ^{100}In, and ^{100}Sn were measured with respect to ^{100}Ag using the GANIL cyclotron, with precisions of 2×10^{-6}, 3×10^{-6}, and 10^{-5}, respectively. [S0031-9007(96)01156-8]

PACS numbers: 21.10.Dr, 27.60.+j

The doubly magic nucleus ^{100}Sn was recently produced and identified in two independent experiments using the projectile fragmentation technique: at GSI with a 1.1 GeV/nucleon ^{124}Xe beam [1] and at GANIL using a 63 MeV/nucleon ^{112}Sn beam [2]. Because of its $N = Z$ character at the double shell closure, it has been keenly sought, and its observation represents the culmination of many years of effort. However, its observation demonstrates only that it is bound against proton decay, whereas a measurement of its mass provides more detailed information on the interaction between protons and neutrons in the same high lying shell model orbits and shell closure near the proton drip line.

The method available for measuring masses of nuclei produced in fragmentation reactions employs time of flight over a linear flight path of ~50–100 m, using high precision magnetic spectrometers (SPEG at GANIL and TOFI at Los Alamos). With currently available count rates, the resolution of these devices is not good enough to perform precise mass measurement of ^{100}Sn. Given the much increased path length when the ions follow a spiral trajectory, we have developed a method using the second cyclotron of GANIL (CSS2) as a high precision spectrometer. The mass resolution obtained with the simultaneous acceleration of $A/q = 3$ light ions (^{6}He, ^{9}Li) was shown to be 10^{-6} [3].

In the present work, neutron-deficient $A = 100$ nuclei were produced via the fusion-evaporation reaction ^{50}Cr + ^{58}Ni at 255 MeV, which is known to be very favorable for the production of nuclei around ^{100}Sn [4]. The highest cross section is for the production of ^{100}Ag, followed by ^{100}Cd, ^{100}In, and finally ^{100}Sn. The $A = 100$ isobars were accelerated simultaneously and detected inside the cyclotron using a silicon detector telescope (ΔE 35 μm, E 300 μm) mounted on a radial probe which can be moved from the injection radius (~1250 mm) up to the extraction radius (~3000 mm). The mass resolution achieved with these heavy ions was of the order of 3×10^{-5}. Using the mass of ^{100}Ag as a reference, the masses of ^{100}Cd, ^{100}In, and ^{100}Sn could be determined with precisions (depending on the statistics) of 2×10^{-6}, 3×10^{-6}, and 10^{-5}, respectively.

Details of the method have already been published [3,5,6], so here we will concentrate on features specific to the present work. For two nuclei, masses m and $m + \delta m$, accelerated simultaneously in CSS2, the separation in time, δt, after N_T turns is given to first order by

$$\delta t/t = \delta m/m\,, \tag{1}$$

where $t = N_T h_2/f$ is the total transit time, h_2 is the CSS2 harmonic, and f is the frequency of the accelerating voltage. This relation is the basis of the calibration procedure: the unknown mass $m + \delta m$ can be determined from the well known reference mass m if the number of turns N_T or the total time of flight t are known. The time of flight, or phase (one RF period being equal to 360°), of the detected ions was measured relative to the RF signal of the CSS2 cyclotron.

After tuning the cyclotron with the primary beam degraded to the appropriate $B\rho$ value [5,6], secondary ions with $A = 100$ and $q = 22^+$ were injected in CSS2. The predicted fractional mass/charge difference between ^{100}Sn^{22+} and ^{100}Ag^{22+} is 2.3×10^{-4} [7], and therefore ^{100}Ag^{22+}, ^{100}Cd^{22+}, ^{100}In^{22+}, and ^{100}Sn^{22+} are simultaneously accelerated to maximum radius in CSS2 [3]. However, with increasing radius, the phase of ions other

 © 1996 The American Physical Society

than $^{100}Sn^{22+}$ (isochronous ions, characterized by constant phase with increasing radius) moves farther and farther ahead of the isochronous phase.

Figure 1(a) shows an accumulations of total energy versus phase spectra for ions with $A = 100$ and $q = 22^+$ acquired with the radial probe at several positions near maximum radius in CSS2. Note that the increasing phase corresponds to smaller time of flight and thus to smaller mass. To aid the interpretation of this spectrum, a simulation of the ion trajectories in the cyclotron has been performed, and is shown in Fig. 1(b). This simulation incorporates the observation that the tuning of isochronism with the degraded primary beam resulted in a phase of $-10°$ close to the extraction radius. Thus $^{100}Sn^{22+}$ is expected around $-10°$ and lighter nuclei are detected at larger phases, proportional to their fractional mass/charge differences. For the $^{100}Ag^{22+}$ ions, which are farthest from isochronism, portions of several turns are intercepted by the detector at a given radius. For ions closer to isochronism, the spread in energies or radii for a single turn are less and fewer turns are intercepted at a fixed radius. These features are clearly visible in Fig. 1(a). Several turns of the prolifically produced ^{100}Ag ions may be seen, and ^{100}Cd are also evident. The intensities of ^{100}In and ^{100}Sn ions are not high enough for them to be readily apparent in this plot. There is a cluster of events with the correct energies and phases to be ^{100}Sn ions, but there is also a comparable number of background events with the correct phases but lower energies. These background events could be attributed mainly to a tail of ^{100}Ag. In order to separate genuine ^{100}Sn events from background, a particle identification parameter $f(Z)$, proportional to the atomic number Z, was derived from a linear combination of the signals from the two detectors of the silicon detector telescope. The coefficients were determined empirically from the data by varying the total energy of the products detected in the silicon detector telescope (related to the radial position of the probe). On this identification parameter we were able to mark off the regions where the bulk of each ion species is to be found. Around phase $-10°$ where the ^{100}Sn events are expected, we could attribute a scattered background of events coming from the Ag and Cd regions of $f(Z)$, very few from the In region, and several events from the Sn region. Figure 2 shows total energy versus phase plots for events falling within the In and Sn windows set on the identification parameter $f(Z)$ and their projections on to the phase axis. Note that the background events that were visible in Fig. 1(a) have disappeared. There is an excess of 10–12 events in the Sn spectra of Fig. 2 around $-10°$ which have correct phase, total energy, and $f(Z)$ values simultaneously, and these are attributed to $^{100}Sn^{22+}$ ions. Note that the bulk of the events in both the In and Sn spectra are due to tails of the much more intense ^{100}Ag and ^{100}Cd groups.

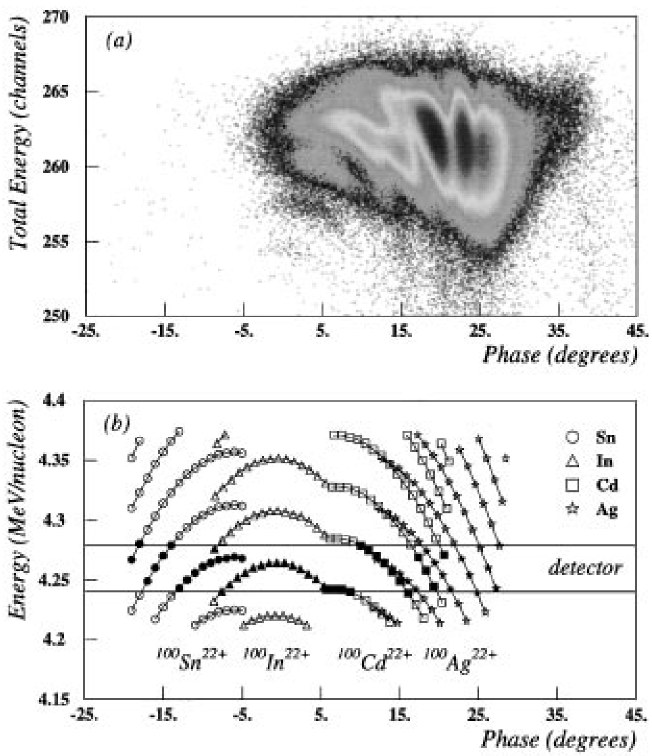

FIG. 1. Energy versus phase spectra accumulated over different positions of the radial probe close to the extraction radius. (a) Experimental spectrum in which the several adjacent orbits intercepted for the most produced ions ($^{100}Ag^{22+}$ and $^{100}Cd^{22+}$) are clearly visible. (b) Result of a simulation for the simultaneous acceleration of $^{100}Sn^{22+}$, $^{100}In^{22+}$, $^{100}Cd^{22+}$, and $^{100}Ag^{22+}$ (without any correction for relative production rates). The cut of the detector (located at a given radius) is indicated by black symbols between the two horizontal lines.

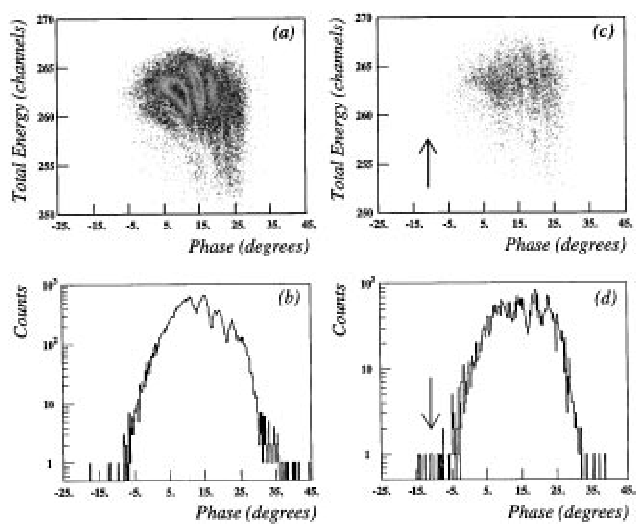

FIG. 2. Total energy versus phase spectra and their projections on to the phase axis, both gated by the identification parameter $f(Z)$ for In [(a), (b)] and Sn [(c), (d)] regions, respectively. The arrows indicate the location of $^{100}Sn^{22+}$ counts (see text).

The relative intensities of these Ag and Cd events in the In and Sn spectra, respectively, differ by a factor of 10. If it is assumed that the background near $-10°$ is due to Ag and Cd ions, then this background would be expected to scale accordingly. Since there are only 4 background counts in the In spectrum, the expected background in the Sn spectrum is therefore no more than 1 count.

In order to determine the masses of the various isobars it is necessary to determine their centroids in phase. This was accomplished using an iterative procedure to subtract the Ag contribution from the Cd spectrum, the Ag and Cd contributions from the In spectrum, and the Ag, Cd, and In contributions from the Sn spectrum to arrive at fairly pure spectra (in the anticipated region of phase) for each of the four isobars, from which the centroids could be determined. The number of turns before detection, N_T which was required to turn the time differences between the various isobars and ^{100}Ag into mass differences, according to Eq. (1), was determined in a separated measurement at the conclusion of the experiment. Finally, we arrive at the following mass excesses:

$$\text{M.E.}(^{100}\text{Cd}) = -74.180 \pm 0.200(\text{syst})\ \text{MeV},$$

$$\text{M.E.}(^{100}\text{In}) = -64.650 \pm 0.300(\text{syst}) \pm 0.100(\text{stat})\ \text{MeV},$$

$$\text{M.E.}(^{100}\text{Sn}) = -57.770 \pm 0.300(\text{syst}) \pm 0.900(\text{stat})\ \text{MeV}.$$

The systematic uncertainties take account of the uncertainties in the subtraction procedure described above. We supposed that there were no long-lived isomeric states. These masses are to be compared with the experimental values presented in the Audi-Wapstra mass table [7] for ^{100}Cd(-74.310 ± 0.100 MeV) [8] and also for ^{100}In(-64.130 ± 0.380 MeV) which was obtained from the combination of an indirect measurement [9] and our previous direct measurement using the CSS2 cyclotron technique [10]. The mass of ^{100}Sn(-56.860 ± 0.430 MeV) given in the Audi-Wapstra mass table is an estimate based on extrapolating systematic trends. Our mass of ^{100}Cd is in good agreement with the existing measurement, which gives good confidence in the new results for ^{100}In and ^{100}Sn.

It is of interest to compare our experimental count rates to statistical model calculations. The absolute transmission of CSS2 is difficult to determine [3]. However, if we suppose that the mean charge distribution for different isobars is centered approximately at the same value (which could be wrong, e.g., if delayed Auger electron emission changed strongly the charge state after the target), we can obtain relative cross sections. To our knowledge, only one value has been measured [11] for ^{100}Ag, which is 3.9 mb. This value is 1 order of magnitude lower than estimations from statistical model calculations that we used previously to estimate the absolute cross section. If we normalize our count rates to this experimental value [11] for ^{100}Ag, we obtain the cross sections of Table I, all of which are 1 order of magnitude lower than the statistical model predictions. Note that the small 40 nb cross section for ^{100}Sn is nonetheless 3 orders of magnitude larger than the ones in fragmentation reactions [1,2].

We compared the shell model calculations of Johnstone and Skouras [12] to the Audi-Wapstra mass table [13] for the binding energies of 33 isotones, $N = 50$, 51, and 52, from ^{90}Zr to ^{102}Sn (see Fig. 3). The calculated binding energies are in good agreement with the mass table values as far as experimental data are available (right side of the dashed vertical line, up to ^{98}Ag and ^{100}Cd), but there is a clear disagreement when the mass table values are derived by extrapolating systematic trends (left side of the line). We added on the same graph our experimental results for ^{100}Cd, ^{100}In, and ^{100}Sn (represented by black stars). As is visible, the shell model calculations agree well with our results, predicting a stronger binding energy than the extrapolations from systematics. At the moment, it is difficult to determine the possible origin of this overbinding. For lighter $N = Z$ nuclei, a strong overbinding is observed and can be attributed to a Wigner term. In a recent work [14], it was shown that this term corresponds to a SU(4) symmetry. It is expected that this term will decrease due to SU(4) symmetry breaking by Coulomb interaction and high angular momenta. It decreases from about 4 MeV around $Z = 8$, to 1.7 MeV in ^{56}Ni. It is an interesting question up to which mass number A this symmetry persists. We hope that the present data and other data on midshell nuclei presently being analyzed will contribute to answer this question. Calculations over a larger domain

TABLE I. Experimental cross sections of the present work normalized to the value of Schubart *et al.* [11] for ^{100}Ag, and compared to statistical model calculations.

	Present work (counts/h nAe)	Present work (mb)	Stat. model PACE (mb)	Stat. model HIVAP (mb) [4,15]	Stat. model CASCADE (mb)
^{100}Ag	~40	3.9 [11]	30	38	38
^{100}Cd	~10	~1	16	7	3.2
^{100}In	~0.01	~0.001	0.02	0.014	0.027
^{100}Sn	$\sim 4 \times 10^{-4}$	$\sim 4 \times 10^{-5}$	···	0.0003	···

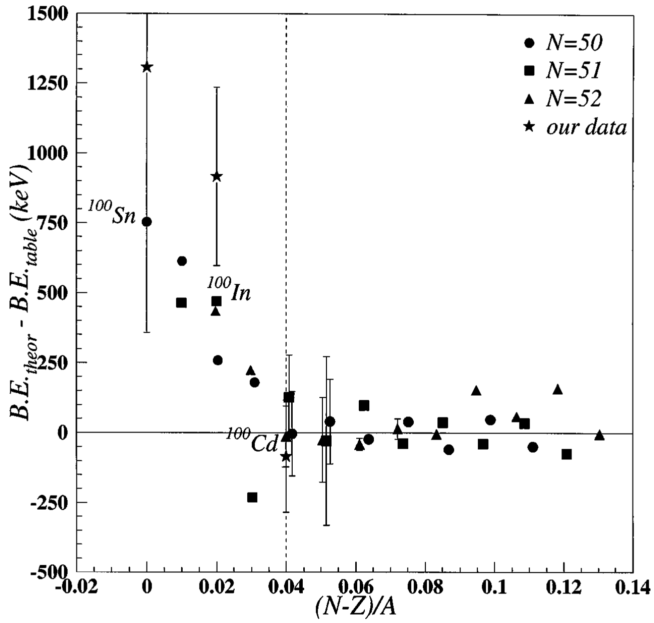

FIG. 3. Comparison between the shell model calculations of Johnstone and Skouras [12] (B.E.$_{\text{theor}}$) and the mass table of Audi and Wapstra [13] (B.E.$_{\text{table}}$) for the binding energies of isotones $N = 50$, 51, and 52 from ^{90}Zr to ^{102}Sn (see text). Our experimental results are represented by black stars.

around $N = Z = 50$ would be desirable, too, in order to disentangle different effects.

In conclusion, ^{100}Sn has been observed as the product of a fusion-evaporation reaction for the first time using the CSS2 cyclotron of GANIL as an efficient high precision mass spectrometer. The masses of not only ^{100}Sn, but also ^{100}In and ^{100}Cd were determined using ^{100}Ag as a reference. The known mass excess of ^{100}Cd has been confirmed within 2×10^{-6}, and we measured for the first time the masses of ^{100}In and ^{100}Sn with a precision of 3×10^{-6} and 10^{-5}, respectively. A preliminary production cross section of 40 nb has been determined for the fusion-evaporation reaction ^{50}Cr + ^{58}Ni $\rightarrow$ ^{100}Sn at 255 MeV.

[1] R. Schneider *et al.,* Z. Phys. A **348**, 241 (1994).
[2] M. Lewitowicz *et al.,* Phys. Lett. B **322**, 20 (1994).
[3] G. Auger *et al.,* Nucl. Instrum. Methods Phys. Res., Sect. A **350**, 235 (1994).
[4] E. Roeckl (private communication).
[5] G. Auger *et al.,* Nouv. GANIL **54**, 7 (1995).
[6] M. Chartier *et al.,* Act. Phys. Pol. B **27**, 451 (1996).
[7] G. Audi and A. H. Wapstra, Nucl. Phys. **A595**, 409 (1995).
[8] K. Rykaczewski *et al.,* Z. Phys. A **332**, 275 (1989).
[9] J. Szerypo *et al.,* Nucl. Phys. **A584**, 221 (1995).
[10] A. Lépine-Szily *et al.,* in *Proceedings of ENAM 95 Conference, Arles, France, 1995,* edited by M. de Saint Simon and O. Serlin Editions Frontières.
[11] R. Schubart *et al.,* Z. Phys. A **352**, 373 (1995).
[12] I. P. Johnstone and L. D. Skouras, Phys. Rev. C **51**, 2817 (1995).
[13] G. Audi and A. H. Wapstra, Nucl. Phys. **A565**, 1 (1993).
[14] P. Van Isacker, D. D. Warner, and D. S. Brenner, Phys. Rev. Lett. **74**, 4607 (1995).
[15] K. Rykaczewski (private communication).